This is an *Accepted Manuscript*, which has been through the Royal Society of Chemistry peer review process and has been accepted for publication.

Accepted Manuscripts are published online shortly after acceptance, before technical editing, formatting and proof reading. Using this free service, authors can make their results available to the community, in citable form, before we publish the edited article. We will replace this *Accepted Manuscript* with the edited and formatted *Advance Article* as soon as it is available.

You can find more information about *Accepted Manuscripts* in the **Information for Authors**.

Please note that technical editing may introduce minor changes to the text and/or graphics, which may alter content. The journal's standard **Terms & Conditions** and the **Ethical guidelines** still apply. In no event shall the Royal Society of Chemistry be held responsible for any errors or omissions in this *Accepted Manuscript* or any consequences arising from the use of any information it contains.

Organic & Biomolecular Chemistry

PAPER

New synthesis of phenyl-isothiocyanates *C*-functionalised cyclams. Bioconjugation and ^{64}Cu phenotypic PET imaging studies of multiple myeloma with the te2a derivative

Zakaria Halime,[a] Mathieu Frindel,[a,b] Nathalie Camus,[a] Pierre-Yves Orain,[a] Marie Lacombe,[c] Michel Chérel,[c] Jean-Fraçois Gestin,[c] Alain Faivre-Chauvet[c] and Raphaël Tripier[a,]*

Azamacrocyclic bifunctional chelating agents (BCAs) are essential for the development of radiopharmaceuticals in nuclear medicine and we wish to prove that their bioconjugation by a function present on a carbon atom of the macrocyclic skeleton is a solution of choice to maintain their in vivo inertness. Based on our very recent methodology using a bisaminal template and selective *N*-alkylation approach, a new synthesis of conjugable *C*-functionalised teta, te2a and cb-te2a has been developed. These chelators have indeed a growing interest in nuclear medicine for positron emission tomography (PET) and radioimmunotherapy (RIT) where they show in several cases better complexation properties than dota or dota-like macrocycles, especially with ^{64}Cu or [67]Cu radioisotopes. Chelators are bearing an isothiocyanate grafting function introduced by *C*-alkylation to avoid as much as possible a critical decrease of their chelating properties. The synthesis is very efficient and yields the targeted ligands, teta-Ph-NCS, te2a-Ph-NCS and cb-te2a-Ph-NCS without fastidious work-up and could be easily extended to other cyclam based-BCAs. The newly synthetised te2a-Ph-NCS has been conjugated to an anti mCD138 monoclonal antibody (mAb) to evaluate its in vivo behavior and potentiality as BCA and to explore a first attempt of PET-phenotypic imaging in multiple myeloma (MM). Mass spectrometry analysis of the immunoconjugate showed that up to 4 chelates were conjugated per 9E7.4 mAb. The radiolabeling yield and specific activity post-purification of the bioconjugate 9E7.4-CSN-Ph-te2a were $95 \pm 2.8\%$ and 188 ± 27 MBq/mg respectively and the immunoreactivity of [64]Cu-9E7.4-CSN-Ph-te2a was 81 ± 7 %. Animal experiments were carried out on 5T33-Luc(+) tumor bearing mice, either in subcutaneous or orthotopic. To achieve PET imaging, mice were injected with [64]Cu-9E7.4-CNS-Ph-te2a and acquisitions were conducted 2 and 20 h post-injection (PI). A millimetric bone uptake was localised in a sacroiliac of a MM orthotopic tumor. Nonspecific uptakes were observed at 2 h PI but, unlike for the tumor, a significant decrease was observed at 20 h PI which improves the contrast of the images.

Introduction

Among the range of potentially useful metals in nuclear medicine, copper has been receiving much interest due to the existence of several radionuclides with different half-life and emission properties that make them suitable for diagnostic imaging or therapeutic applications, as well as to the improvement of the availability of most of these nuclides.[1,2]

The most interesting radionuclides are the hardly available [67]Cu ($t_{1/2}$ = 62.0 h, β^- 100%, E_{max} = 0.577 MeV, γ 16%, E_{max} = 0.093 MeV, γ 48%, E_{max} = 0.185 MeV) for vectorised radiotherapy purposes and the now widely available [64]Cu ($t_{1/2}$ = 12.7 h, β^+ 17.4 %, E_{max} = 0.656 MeV, β^- 39.6 %, E_{max} = 0.573 MeV) for positron emission tomography (PET).[1,2] According to its radiophysical properties, ^{64}Cu seems to be a radionuclide of choice to investigate PET-phenotypic imaging.
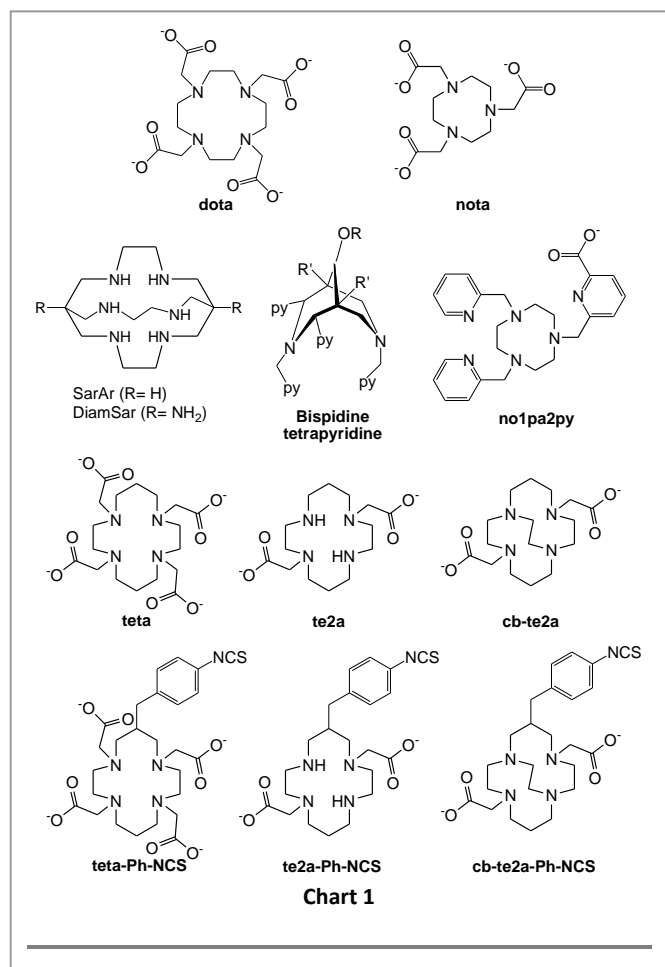
Tetraazamacrocycles are known as efficient chelating agents for numerous metal ions.[3] Owing to the presence of secondary amine functions, these macrocycles can be *N*-functionalised with various coordinating groups, which allow the preparation of a wide range of ligands suitable for the development of metal-based imaging and therapeutic agents in medicine. In particular, the use of the well-known commercially available dota (1,4,7,10-tetraazacyclododecane-1,4,7,10-tetraacetic acid) (Chart 1) and its bifunctional derivatives is now admitted in numerous cases since they form thermodynamically stable and inert chelates. However, the ubiquitous dota is misused in many applications such as a copper chelate for PET and RIT applications respectively with [64]Cu

This journal is © The Royal Society of Chemistry 2015

Org. Biomol. Chem., 2015, 00, 1-3 | 1

Organic & Biomolecular Chemistry

Chart 1

and [67]Cu.[4-8] It is now accepted that dota and its conjugable analogues are not the optimal ligands for ^{64}Cu complexation for in vivo applications. Indeed, this ligand does not fulfil all the criteria required, that includes the need to combine a high thermodynamic stability and kinetic inertness of the complexes (especially in its reduced Cu(I) form) with a fast metal complexation under mild conditions. For these reasons, increasing interest is now directed towards other azamacrocycles such as SarAr,[9-11] nota[12-14] and other chelators like bispidyne ligands[15]. In particular, *N*-functionalised cyclams such as acetate,[16-18] phosphonate,[19-21] picolinate[22-24] derivatives are now often preferred to dota because of their favorable coordinating properties with Cu(II). If we only look at the simplest ligands, teta or te2a (Chart 1) form Cu(II) complexes with very high thermodynamic stability[25-27] while cb-te2a provides complexes with exceptional inertness,[28] which prevents their dissociation following either an acid-catalysed pathway or a reduction of Cu(II) to Cu(I).[29,30] Other cyclam derivatives such as picolinate compounds te1pa[22] and cb-te1pa[24] are also very promising.

However, cyclam bifunctional chelating agents (BCA) analogues, with an additional specific group able to form a stable bond with specific biomolecular vectors are not easily accessible. The best methodology appears to be the introduction of the specific anchoring function via a carbon atom of the macrocyclic structure. Compared to other methods based on the sacrifice and the transformation of one of the chelating arms of the macrocycle into anchoring function or the use of very difficult procedures to

synthesise bifunctional arms (arm bearing both the chelating function and the conjugable function),[31-35] the so called *C*-functionalisation approach has proved to be more efficient in terms of preserving the coordination properties of the ligands.[36-38] Additionally, even if teta-Cu or dota-Cu complexes are hexadentate and that two arms of the ligands are free for conjugation, the grafting of such chelates don't conserve the overall charge of the complex and the selective activation of only one carboxylic function is quasi-impossible leading to multi-linked chelates.

The addition of the well-known phenyl isothiocyanate conjugable function on the macrocyclic backbone then remains a challenging task and only BCA derivatives teta-Ph-NCS[39-40] and cb-te2a-Ph-NCS[11] have been described (Chart 1). These two BCA were prepared following very fastidious synthetic methodologies which are not extendable to the preparation of other cyclam based ligands such as te2a. Today, te2a, which was described by D. Pandya and coworkers as an efficient copper chelator for PET imaging, has no "graftable" *C*-functionalised analogue and the only vectorisation studies have been conducted using one of the two acetate chelating functions for conjugation.[41]

Knowing the importance of such cyclam BCAs, we recently reported a new methodology leading to the synthesis of specifically *C*-functionalised analogues of teta, te2a and cb-te2a bearing an ethylhydroxy function.[42,43] This synthesis is based on an initial preorganisation of the tetraamine N,N'-Bis(2-aminoethyl)-1,3-propanediamine (232) using the glyoxal (compound **1**, scheme 1) as an organic template followed by a cyclisation step with an α,β unsaturated ester functionalised in the α position of the carbonyl group. We also showed that this reactivity can be extended to other cyclising agents such as methyl 2-(4-nitrobenzyl) acrylate (compound **2**, scheme 1). The nitrobenzyl group is well known as a precursor of an aniline moiety and can be easily transformed into the desirable phenyl isothiocyanate function. However, the replacement of ethylhydroxy function by nitrobenzyl group implies modifications of the macrocycle behavior and reactivity, which is why we dedicated the first part of this work to the adaptation of our previously described methodology to the presence of the nitrobenzyl group in order to elaborate a convergent, direct and efficient synthetic pathway for the preparation of very attractive bifunctional chelators analogues with a great importance in the field of nuclear medicine. In order to simplify this preliminary work and before going toward more complex and attractive phosphonate[19-21] or picolinate[22-24] ligands, we chose to extend our new methodology to the synthesis of the previously described teta-Ph-NCS[44-46] and cb-te2a-Ph-NCS[18,47] and the never before described te2a-Ph-NCS (Chart 1).

Unlike teta-Ph-NCS and cb-te2a-Ph-NCS, the new BCA te2a-Ph-NCS has never been conjugated to a biovector for PET application. Therefore, as a first step in our research, we decided to carry out the first bioconjugation of te2a-Ph-NCS in order to evaluate the input of the use of *C*-functionalisation to introduce the conjugation function (Ph-NCS) by comparison to the free te2a or its analogue previously conjugated to biovector through one of the acetate arms. The choice of te2a-Ph-NCS was also motivated by the milder conditions needed for radiolabeling. Because unlike cb-te2a derivatives which have proton sponge behavior resulting in a very slow metalation kinetic and a requirement for elevated

2 | *Org. Biomol. Chem.* 2015, **00**, 1-3

This journal is © The Royal Society of Chemistry 2015

Organic & Biomolecular Chemistry

ARTICLE

temperatures for radiolabeling, te2a derivatives can be radiolabeled at room temperature which is more compatible with the use of fragile biomolecules such as antibodies.

For such a study we have had the opportunity to explore for the first time PET-phenotypic imaging of 5T33 Multiple Myeloma (MM) tumor bearing mice. MM is a malignant plasma cell disorder characterised by the proliferation of clonal cells in the bone marrow and at later stages of the disease in extramedullary sites, with the subsequent production of a plasma monoclonal immunoglobulin. Currently, no consensual imaging protocol exists, this includes MRI (Magnetic Resonance Imaging), CT (Computed Tomography), radiography and PET imaging. Even if ^{18}F-FDG (^{18}F-fluorodeoxyglucose) PET imaging can be useful, the sensitivity and the specificity of this radiopharmaceutical are low in MM disease, notably due to the diffuse bone marrow involvement and variability in metabolic status in function of disease staging.[48] Phenotypic imaging is a promising tool based on the visualisation of the overexpressed CXCR4 receptors or the constant expression of CD38/CD138 antigene that can be suitably combined with PET imaging. To be successful, this strategy needs to combine the right components in order to prepare an efficient radiopharmaceutical which includes a specific biovector and a selective chelator capable of safely carrying the appropriate radionuclide.

Thus, in this work, te2a-Ph-NCS cyclam derivative was conjugated to an anti mCD138 monoclonal antibody (mAb) and studied in vitro as well as in vivo using PET-imaging.

Results and Discussions

Ligand Synthesis. Our strategy consists of the cyclisation of the preorganised tetraamine **1** (Scheme 1)**,** obtained by condensation of the starting tetraamine 232 and glyoxal, in its *cis*-bisaminal intermediate form, with the methyl acrylate derivative **2**.
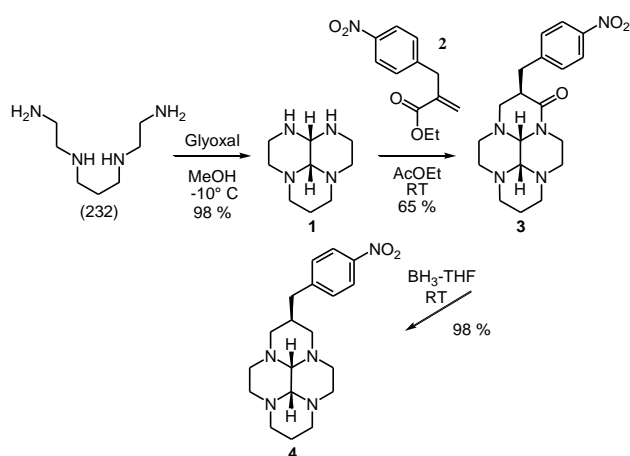

Scheme 1. Three steps synthesis of the bisaminal cyclam nitrobenzyl: template effect, cyclisation and reduction

As it was fully described in our previous work,[42,43] the *C*-functionalised macrocycle **3** was obtained with 65 % yield without fastidious purification steps since the desired compound precipitates during the reaction where acetonitrile, previously described as the reaction solvent, was replaced in this work by ethylacetate. In these conditions, the oxo-macrocycle was obtained in its specific *syn-cis* configuration that will permit both an easy deprotection of the bisaminal bridge and the control of the regiospecificity in the following synthesis steps.[42,43]

The nitrobenzyl group is of course the protected precursor of an aniline moiety which will evolve into a conjugable thioisocyanate function. Since the mono-*N*-functionalisation of the macrocycle was not the goal of this work, compound **3**, which is yet a precursor of mono-alkylated cyclams, is reduced with borane tetrahydrofuran to give **4** with 98 % yield. One has to note that, compared to our previous work where $NaBH_4$ was used to reduce the oxo group, in this case the use of the stronger reducing agent BH_3-THF was necessary to obtain compound **4**. This reaction is performed at room temperature to avoid the reduction of the nitrobenzyl group which can be inconvenient for the following reaction steps.

The *C*-functionalised "protected" macrocycle **4** is the keystone intermediate of our synthesis since all the bisaminal chemistry can be applied to generate both regiospecific *N*-functionalised or cross-bridged compounds. For this purpose, 10 equiv. benzyle bromide were added to **4** in dry acetonitrile to form the expected *trans*-di-*N*-alkylated salt **5**, which was obtained as a white precipitate with 93 % yield (Scheme 2).
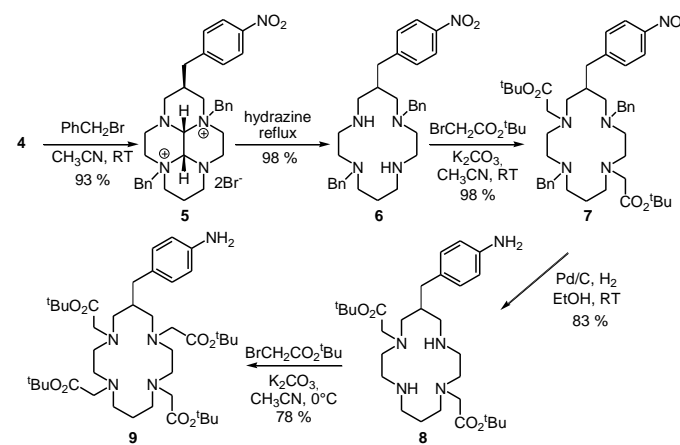
Scheme 2. Selective protection of cyclams BCA's

The total deprotection of the bisaminal bridge of compound **5** was performed using hydrazine monohydrate to give the di-*N*-benzylcyclam derivative **6** with 98 % yield. Compound **6** can then be considered as a precursor of *trans*-difunctionalised cyclam-based ligands; thus, we functionalised this compound with acetate arms in order to obtain *C*-functionalised te2a and then teta BCA analogues. The alkylation of the secondary amine functions of **6** by *tert*-butyl bromoacetate led to dibenzyl te2a[t]Bu-Ph-NO$_2$ **7** with near quantitative yields. The subsequent reductive treatment **7** with Pd-catalysed hydrogenolysis led to both the removal of *N*-benzyl protecting groups and the reduction of the nitrobenzyle into an

This journal is © The Royal Society of Chemistry 2015

Org. Biomol. Chem. 2015, **00**, 1-3 | **3**

aniline function. Compound te2a^{t}Bu-Ph-NH$_2$ **8** was then obtained with 83 % yield. This compound was used later as a precursor for the targeted te2a BCA analogue but it can be also used as the teta^{t}Bu-Ph-NH$_2$ **9** precursor by introducing *tert*-butyl bromoacetate groups on the two remaining secondary amine functions. One can underline that, at the reaction temperature of 0 °C, the primary amine function of the aniline moiety does not react with *tert*-butyl bromoacetate, which prevents additional synthetic steps for the specific protection and deprotection of the aniline.
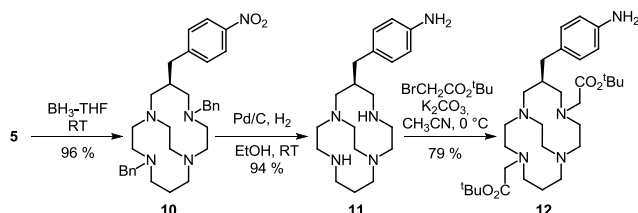

Scheme 3. Reduction of the bisaminal bridge to lead to a cross-bridged cyclam BCA.

The final steps of our strategy consist of the transformation of the *tert*-butyl ester groups into carboxylic acid functions and the activation of the aniline moiety (Scheme 4). The deprotection of the *tert*-butyl ester groups using trifluoroacetic acid in dichloromethane at room temperature gives quantitatively the ligand te2a-Ph-NH$_2$ **13**, as a trifluoroacetate salt. Attempts to perform the hydrolysis of the ester functions using classical conditions (HCl 6M under reflux) resulted in the formation of lactam derivatives due to the reaction of one of the remaining secondary amine functions with the carboxylic groups. This side reaction is promoted by the elevated temperature needed to hydrolyze the ester functions and to evaporate the excess solvent during the work-up of the reaction. No trace of this lactam was observed in the relatively mild reaction and work-up conditions of the hydrolysis using trifluoroacetic acid. The final conjugable BCA te2a-Ph-NCS **14** was then obtained after treatment with thiophosgene following a standard procedure[49] with 87 % yield.

The absence of secondary amines in compounds **9** and **12**, allowed us to classically perform their final quantitative hydrolysis in refluxing HCl 6M to yield teta-Ph-NH$_2$ **15** and cb-te2a-Ph-NH$_2$ **17**. The subsequent activation of both macrocycle was performed as previously described to give te2a-Ph-NCS **14** and cb-te2a-Ph-NCS **18** as white solids with respectively 85 % and 81 % yields. The newly obtained te2a-Ph-NCS **14** was then selected for conjugation, biodistribution and PET imaging studies.

Despite the number of steps, the syntheses are very easy to perform and the overall yields are quite good. Additionally, following a common starting procedure, the present synthetic strategy leads to three different compounds of interest versus only one for the previously described syntheses. The use of a template in our case enables us to avoid the use of highly diluted conditions for the cyclisation step (vs Meares's and al. or Moreau's and al. methods),[39,45,56] which constitutes an important advantage of this new synthesis. Another important advantage of this synthetic strategy is the use of the glyoxal instead of the previously used

butanedione because it is a more robust template end protecting group which gives access to more diverse reactivity.[47] Finally, as demonstrated in our previous works, compound **3** can be used as a precursor for very promising mono-functionalized cyclam BCAs.[42]

In a parallel synthetic pathway, the reduction of the bisaminal bridge of **5** was achieved with BH$_3$-THF to give the cross-bridged cyclam analogue 10 with 96 % yield (Scheme 2). Since literature often reported cross-bridged tetraazamacrocycles as proton sponges, the compound **10** was extracted as a free base from a very basic aqueous solution of potassium hydroxide (pH > 14) using chloroform. The Pd-catalysed hydrogenolysis of compound **10** led in the same time to the hydrogenolyse (debenzylation) and the reduction of the nitrobenzene moiety which gave the corresponding reinforced macrocycle cb-cyclam-Ph-NH$_2$ 11 as a free base with 94% yield. As proposed before, by introducing of *tert*-butyl bromoacetate groups on the two remaining secondary amine functions, cb-te2a^{t}Bu-Ph-NH$_2$ **12** was obtained with 79 % yield.
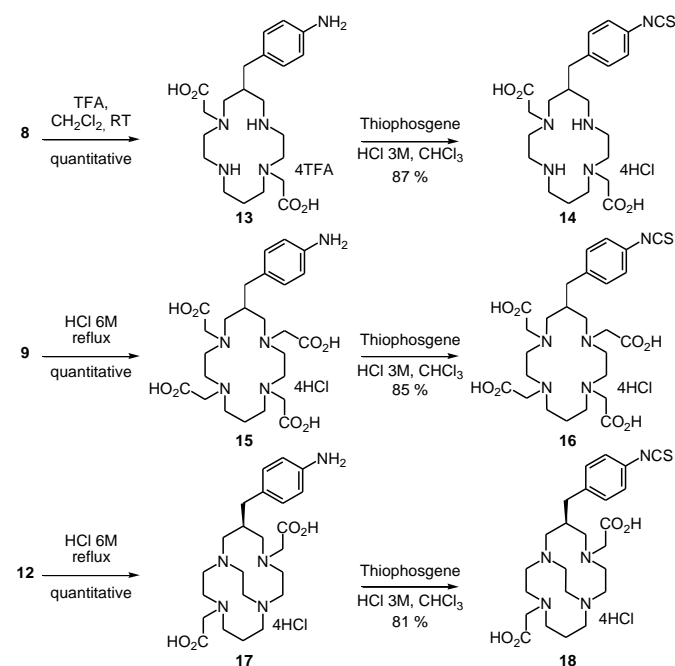
Scheme 4. Synthesis of te2ta-Ph-NCS (**14**), teta-Ph-NCS (**16**) and cb-te2a-Ph-NCS (**18**)

Conjugation, ^{64}Cu radiolabeling of te2a-Ph-NCS and 9E7.4-CSN-Ph-te2a and in vitro stability toward EDTA. The conjugation of the activated te2a-Ph-NCS **14** to the 9E7.4 mAb was performed following the standard protocol described in experimental section. The LC-ESI-MS analysis showed that the signal associated with unreacted 9E7.4 was present in all deconvoluted mass spectra of the reaction mixtures. The ESI mass spectrum of the native unreduced 9E7.4 showed a signal with a mass-to-charge (m/z) value of 147469 Da and an additional signal of 156 480 Da. For the reduced 9E7.4, m/z values were 49533 (main value), 49681 and 24840 Da. Considering the conjugation product (unreduced 9E7.4-CSN-Ph-te2a), m/z values were 147923, 157617 and 157957 Da, whereas the product which has undergone reduction showed

values of 49 999, 50 467 and 24 768. Given these results, the 9E7.4 is conjugated in a range of 0 to 4 chelates per mAb, on heavy chains. One should notice that the analysis of the product following reduction gave more accurate results than the native one. Based on these results, the yield of the conjugation process was evaluated to 10%, which correspond to 2 ligands per antibody. Similar results are reported in the literature for other isothiocyanate derivatives such as SCN-Bz-dota or SCN-Bz-nota using similar protocol.[50,51]

For the in vitro study, the 9E7.4-CSN-Ph-te2a imunoconjugate and the te2a-Ph-NCS BCA (**14**) were radiolabeled with ^{64}Cu at different temperature, time and pH conditions to optimize the procedure. Results are given in tables TS1 and TS4 (see in ESI). No significant difference was observed between pH 5 (acetate buffer) and pH 7 (ammonium acetate) and the radiolabeling yields were quite optimal (78 to 86 % for the immunoconjugate, without further purification) after only 15 min whether at RT or 40 °C. These radiolabeling characteristics obtained for both te2a-Ph-NCS **14** and 9E7.4-CSN-Ph-te2a are comparable to those described in the literature for chelators or mAbs-conjugated ligands radiolabeling with [64]Cu.[52,53]

The radiolabeling results obtained for te2a-Ph-NCS **14** are also quite similar to those previously reported for te2a[7] which confirms that the presence of the benzyl isothiocyanate on the carbon backbone of the macrocycle does not modify the ^{64}Cu radiolabeling proprieties of this chelator. More importantly, unlike in the previous work of Pandya and al., where a significant decrease of the radiolabeling rate was observed when te2a was conjugated to RGDyA peptide through one of the acetate arms,[41] no difference in the radiolabeling rate was observed between the chelator te2a-Ph-NCS **14** and the bioconjugate 9E7.4-CSN-Ph-te2a. This result emphasizes clearly the importance of our *C*-functionalisation strategy for the preservation of the chelator's complexation proprieties even after the bioconjugation.

In vitro competition assays of ^{64}Cu-te2a-Ph-NCS and [64]Cu-9E7.4-CSN-Ph-te2a against EDTA have then been performed to evaluate the relative inertness of the radiolabeled chelator and its corresponding bioconjugate. Results showed that in both cases, 10000 equivalent of EDTA are needed to displace 50 % of ^{64}Cu after one night incubation at RT (see table TS2 in ESI). Unfortunately, in the absence of a similar study for the corresponding non C-functionalized analogue te2a in the literature, we were unable to evaluate the effect of the presence of the benzyl isothiocianate group on the stability of the radiolabeled chelator. Nevertheless, this study clearly shows that the bioconjugation has no negative impact on the radiolabeled chelator stability.

The best condition, i.e. ammonium acetate 0.3 M, pH 7, 40°C and 30 min, has been chosen to radiolabel 9E7.4-CSN-Ph-te2a for in vivo studies that gave a specific activity of 188 ± 27 MBq/mg (28 ± 4 MBq/nmol) with a radiolabeling yield of 95 ± 2.8%. The best specific activity described for ^{64}Cu antibody radiolabeling is 225 MBq/nmol,[54] which is about 10 fold greater than the one we obtained, but the antibody used by Schjoeth-Eskesen et al. has been modified with 3 ligands per antibody and no information was

given about the specific activity of ^{64}Cu chloride starting material. More usually reported specific activities with ^{64}Cu radiolabelled antibodies are comparable to our results.[55,56] Additionally, Compared to the specific activity of the starting ^{64}Cu solution (24.75 MBq/nmol of total copper; 6.8 MBq/nmol of total metallic contaminant), the specific activity obtained with the 9E7.4-CSN-Ph-te2a is also consistent with results obtained by LC-ESI-MS.

Immunoreactivity. Immunoreactive fraction of [64]Cu-9E7.4-CSN-Ph-te2a was 81 ± 7%. This result confirms that the conjugation technic does not alter significantly the recognizing site of 9E7.4 antibody. The small partial loss of immunoreactivity can be explained by random conjugation of the chelate on lysine moieties in or close to the mCD-138 antigen binding site.

PET imaging of multiple myeloma mice model. Overall PET-CT images views and specific sagittal section are presented in Figure 1 and 2 while biodistribution (%ID/g in relevant tissues) extracted from PET-CT images quantification are given in Figure 3. More details on the raw quantitative data of subcutaneous multiple myeloma tumor bearing mice at 2 h and 20 h post-injection (PI) of [64]Cu-9E7.4-CSN-Ph-te2a are given in Table TS3 (in ESI). In parallel control experiment, a complementary and comparative biodistribution study of an iodine-125 radiolabeled 9E7.4, performed in the same mice model[57] was used to evaluate the affinity of the non-te2a-modified 9E7.4 (Figure S43 in ESI). This experiment was used to have a correct comparative study to evaluate the good behavior of our radiopharmaceutical.
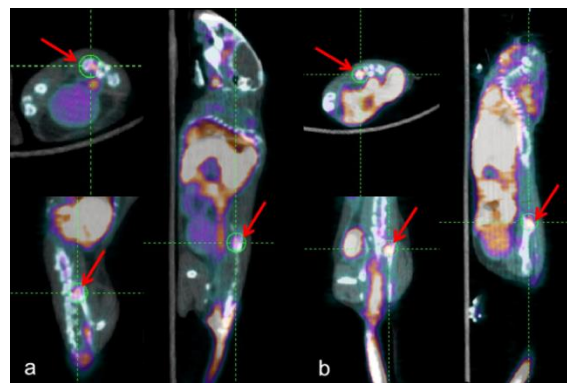
Figure 1. PET-CT images in 3 axes: orthotopic MM tumor bearing mice at 2 h (a) and 20 h (b) PI of [64]Cu-9E7.4-CSN-Ph-te2a. Coronal (top left), transversal (bottom left) and sagittal (right). Tumors are indicated by red arrows.

MM subcutaneous tumor bearing mice showed a mild uptake in the tumor at 2 h post-injection (PI) which demonstrates an in vivo affinity of [64]Cu-9E7.4-CSN-Ph-te2a for mCD-138 (syndecan-1) antigen. This tumor uptake decreases between 2 and 20 h PI from 4.8 to 3.7 %ID/g. Concerning the nonspecific uptakes that can be observed in various tissues, all mice showed high signal in the vascular bed at 2 h PI, especially in the heart, aorta and supra-aortic

trunks. Additionally, high uptakes were observed in the liver and gut at the early time, with a significant clearance of the radioactivity from 2 h to 20 h PI. Thus, tumor to tissues ratios increased significantly between 2 h and 20 h PI from 0.21 to 0.55 for tumor/liver, 0.29 to 1.26 for tumor/heart and 4.3 to 6.7 for tumor/muscle. This difference in the kinetic of the radioactivity clearance between the tumor and the nonspecific tissues allows the visualization of the tumor in near liver area with the radiolabeled bioconjugate [64]Cu-9E7.4-CSN-Ph-te2a even with a low tumor uptake. Fast clearance of radioactivity from liver and gut is not in accordance with the fact that the microvilli of basal hepatocytes express the CD-138 antigen, as it was also confirmed in the biodistribution control experiment using [125]I-9E7.4 in the same mice model (Figure S43 in ESI).
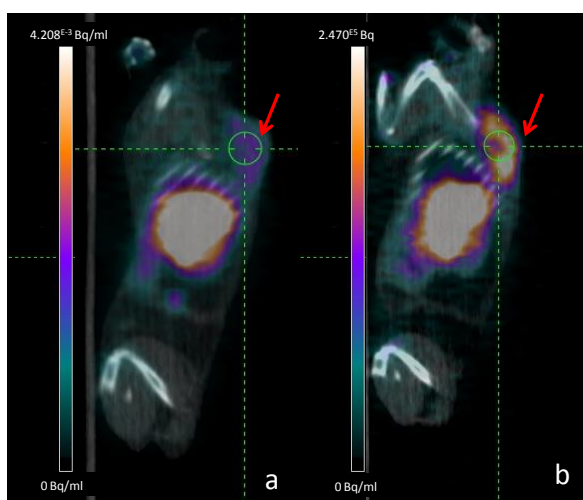

Figure 2. PET-CT images: sagittal section of a dorsal subcutaneous MM tumor bearing mice at 2 h (a) and 20 h (b) PI of [64]Cu-9E7.4-CSN-Ph-te2a. The tumor is indicated by a red arrow.
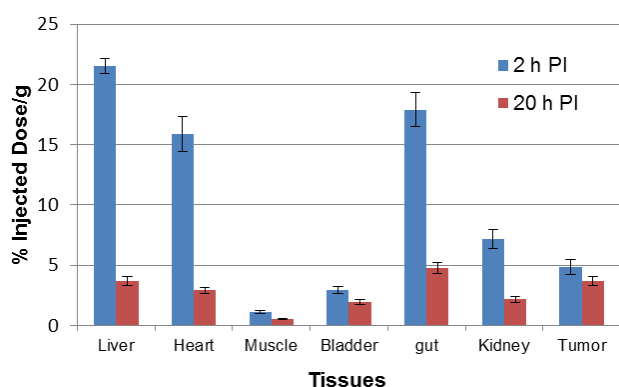

Figure 3. %ID/g extracted from PET-CT image of subcutaneous multiple myeloma tumor bearing mice at 2 h and 20 h post-injection (PI) of [64]Cu-9E7.4-CSN-Ph-te2a. The %ID/g was normalised for a 20 g mice and calculated as follow: %ID/g = ([activity measured in the organ]/[injected activity] $\times$ [mouse weight/20])

Two hypotheses could explain this phenomenon: instability of the ^{64}Cu complex due to a transchelation of the radionuclide to protein involved in copper metabolism[58-60] or a metabolism of the radioimmunoconjugate itself. The first hypothesis seems to agree with the in vitro results but it i not in accordance with the in vivo observations. In fact, in the case of copper release, an increase of liver and gut uptakes should be observed between early and later time PI but at the opposite the liver uptake decreases between 2 and 20 h. Thus, a fast metabolism of the [64]Cu-9E7.4-CSN-Ph-te2a is more coherent with the in vivo observation of a low tumor uptake and a fast body clearance.

Conclusions

The aim of this work was to improve and complete our recent efficient strategy for the synthesis of cyclam based bifunctionalised chelating agents where the supplementary anchoring function is introduced via a carbon atom of the macrocyclic. This kind of BCAs is now well known to allow for the conjugation of macrocycles on biomolecules without affecting their coordination (stability, inertness…) properties as opposed to other procedures where the sacrifice / denaturation of one chelating arm to introduce an anchoring function can lead to a critical loss of their complexation properties and their potential for safe applications in nuclear medicine.

Using a specific Michael acceptor as cyclising agent, a paranitrobenzyl function was directly introduced on the cyclam carbon skeleton in an efficient cyclisation reaction with tetraamine 232 assisted by a bisaminal central template; which overcome the need for highly diluted conditions normally needed for this kind of cyclisation reaction. The compound obtained is the keystone of our synthesis since it gives an easy access to three different bifunctional chelators teta-Ph-NCS, te2a-Ph-NCS and cb-te2a-Ph-NCS relevant to the complexation ^{64}Cu and [67]Cu radionuclides: chelators that are difficult if not almost impossible to obtain following the previously described procedures. The isothiocyanate function bearing chelates can be directly conjugated to biomolecules, especially peptides and antibodies. Another important point is that, compared to other methodologies which lead in general to a single ligand, our synthetic strategy can give access to a large class of ligands of interest based on the *C*-functionalised cyclam skeleton .

Then the newly synthesised te2a-Ph-NCS BCA was conjugated to the monoclonal antibody 9E7.4 (anti mCD138) mAb for a first attempt of phenotypic imaging of Multiple Myeloma in 5T33-Luc(+) tumor bearing mice. The bioconjugation as well as the radiolabeling with ^{64}Cu of the BCA and the bioconjugate were successfully achieved. Moreover, in vitro stability studies showed that, compared to the previous conjugation methodologies, the *C*-functionalisation leads to a better conservation of the chelation properties. PET-imaging study in mice using ^{64}Cu radioimmunoconjugate showed specific uptake in the tumor as well as nonspecific uptakes mainly in the liver, gut and vascular bed at 2 h PI but the significant decrease in the nonspecific uptake at 20 h PI improves considerably the imaging contrast. Of course for a future work, several parameters can be optimised which leaves plenty of

room for the improvement of such applications. Nevertheless, as first PET phenotypic images in orthopic model of MM, this work represents an encouraging example of PET imaging using *C*-functionalised cyclam ^{64}Cu chelates and shows that radiopharmaceuticals can be redesigned for a specific targeted pathology. This redesigning can be achieved by modifying the type of the biovector and/or the nature of the cyclam *N*-functionalisation (acetate, phosphonate, picolinate… arm(s)). Taking advantage of the efficiency and adjustability of our synthesis, our efforts are currently directed toward this goal.

Experimental Section

Materials and Methods. Bisaminals **1** and **2** were synthesised as previously described. 2D NMR [1]H-^{1}H homonuclear, [1]H-^{13}C and [1]H-^{15}N heteronuclear correlations and homonuclear decoupling experiments were used for assignment of the ^{1}H and ^{13}C signals. The δ scales are relative to TMS (^{1}H, ^{13}C) and CH_3NO_2 (^{15}N). The signals are indicated as follows: chemical shift, intensity, multiplicity (s, singlet; br s, broad singlet; d, doublet; t, triplet; m, multiplet; q, quartet), coupling constants *J* in hertz (Hz), assignment: Hα, Cα and Hβ, Cβ correspond to CH or CH_2 located in alpha or beta position respectively of considered nitrogen atom; Am, Ar and Ph are the abbreviations used for aminal, aromatic and phenyl respectively). All analytical spectra and data are given in Supplementary Information.

Compound 4. A 1 M solution of borane tetrahydrofuran (100 ml) was added to previously described[42,43] compound **3** (4 g, 1.07x10^{-2} mol) under nitrogen. After 18 hours stirring at ambient temperature, the reaction was quenched using first methanol then water. The white solid obtained after solvents removal under reduced pressure was dissolved in 100 ml of 3 M solution of hydrochloric acid and refluxed for one hour. After cooling down to room temperature, the reaction mixture was neutralised using potassium hydroxide pellets. Finally, compound **4** was obtained as off-white crystals (3.75 g, 98 %) after a liquid-liquid extraction at pH 14 using dichloromethane (3 x 250 ml) followed by drying over $MgSO_4$ and solvents removal under reduced pressure. ^{1}H NMR (300 MHz, CDCl₃, 25 °C, TMS): δ (ppm) = 8.12 (d, *J* = 8.8 Hz, 2H, C*H*-Ar), 7.26 (d, *J* = 8.8 Hz, 2H, C*H*-Ar), 4.49-3.39 (m, 2H), 3.08 (d, *J* = 3.0 Hz, 1H, N-C*H*-N), 2.99 (d, *J* = 3.3 Hz, 1H, N-C*H*-N), 2.91-1.73 (m, 17 H), 1.41 (bs, 1H), 1.20 (d, *J* = 12.0 Hz, 1H). ^{13}C Jmod NMR (75 MHz, CDCl₃, 25 °C, TMS): δ (ppm) = [147.4, 146.7] (*C*-Ar), [129.6, 123.8] (*C*H), [77.0, 76.9] (N-*C*H-N), 61.8 (CH_2-Ph), [58.6, 56.1, 54.4, 52.6, 45.8, 44.8, 38.4] (CH_2-α-N), 30.3 (*C*H-β-N), 19.7 (CH_2-β-N). HRMS (ESI) *m/z* calcd for $C_{19}H_{28}N_5O_2^+$ [M+H]⁺: 358.2243; found: 358.2238.

Compound 5. A solution of benzyl bromide (3.33 mL, 27.98 mmol) in distilled CH_3CN (10 mL) was added dropwise to a solution of compound **4** (1.00 g, 2.80 mmol) in distilled CH_3CN (25 mL). The solution was stirred at ambient temperature for 10 days, then the precipitate formed during the reaction was isolated by filtration. The solid was washed with CH_3CN (2 × 10 mL) then with Et₂O (2 × 10 mL) and finally dried under vacuum to give **5** as a white powder

(1.82 g, 93%). ^{1}H NMR (300 MHz, DMSO-d[6], 25 °C, TMS): δ (ppm) = 8.17 (d, *J* = 5.4 Hz, 2H, C*H*-Ar), 7.68-7.54 (m, 10H, C*H*-Ar), 7.48 (d, *J* = 5.4 Hz, 2H, C*H*-Ar), 5.53 (d, *J* = 18 Hz, 2H), 5.34 (d, *J* = 7.8 Hz, 1H), 5.23 (d, *J* = 7.8 Hz, 1H), 4.99 (d, *J* = 7.8 Hz, 2H), 4.26 (t, *J* = 5.4 Hz, 2H), 3.71-2.48 (m, 17H), 2.14-2.06 (m, 1H), 1.81 (d, *J* = 8.7 Hz, 1H). ^{13}C Jmod NMR (75 MHz, DMSO-d[6], 25 °C, TMS): δ (ppm) = [146.3, 145.7] (*C*-Ar), [133.5, 133.4, 130.7, 130.6, 130.3, 129.1, 129.0] (*C*H-Ar), [126.0, 125.9] (*C*-Ar), [123.5] (*C*H-Ar), [75.0, 74.9] (N-*C*H-N), [62.7, 60.8, 60.6] (CH_2-Ph), [59.4, 55.3, 50.2, 46.9, 46.1, 46.0, 35.6] (CH_2-α-N), 29.3 (*C*H-β-N), 18.0 (CH_2-β-N). HRMS (ESI) *m/z* calcd for $C_{33}H_{41}N_5O_2^{2+}$ [M]²⁺: 269.6630; found: 269.6625.

Compound 6. Compound **5** (5 g, 7.15 mmol) was dissolved in hydrazine monohydrate (30 mL, 64% in water) then the reaction mixture was refluxed for 4 hours. After cooling down to room temperature the product precipitated then the excess of hydrazine was eliminated by filtration. The precipitate was dissolved in distilled H_2O (30 mL) and the product was extracted with CH_2Cl_2 (3 × 100 mL). The organic fractions were dried over $MgSO_4$, filtrated and evaporated under reduced pressure to give **6** (3.6 g, 98 %) as a yellow solid. ^{1}H NMR (300 MHz, CDCl₃, 25 °C, TMS): δ (ppm) = 8.00 (d, *J* = 6.0 Hz, 2H, C*H*-Ar), 7.28-7.06 (m, 12H, C*H*-Ar), 3.89-3.76 (m, 2H), 3.41-3.33 (m, 2H), 2.14-2.06 (m, 20H), 1.58 (bs, 1H). ^{13}C Jmod NMR (75 MHz, CDCl₃, 25 °C, TMS): δ (ppm) = [148.2, 146.0, 137.1, 136.2] (*C*-Ar), [129.6, 128.9, 127.8, 126.8, 126.7, 123.1] (*C*H-Ar), [58.1, 57.8, 57.4] (CH_2-Ph), [55.0, 54.1, 53.4, 51.9, 50.1, 47.7, 47.3, 38.4] (CH_2-α-N), 36.8 (*C*H-β-N), 25.46 (CH_2-β-N). HRMS (ESI) *m/z* calcd for $C_{31}H_{42}N_5O_2^+$ [M+H]⁺: 516.3339; found: 516.3333.

Compound 7. A solution of *tert*-butyl bromoacetate (573 μL, 3.88 mmol) was added to a suspension of compound **6** (1 g, 1.94 mmol) and K_2CO_3 (1.07 g, 7.76 mmol) in distilled CH_3CN (80 mL). After 24 hours stirring at ambient temperature, the reaction mixture was filtrated and then the solvent was evaporated under reduced pressure. Finally, The resulting yellow oil was purified by flash chromatography on silica gel (CHCl₃/MeOH, 99:1-98:2) to give **7** as yellow oil (1.42 g, 98 %). ^{1}H NMR (300 MHz, CDCl₃, 25 °C, TMS): δ (ppm) = 8.02 (d, *J* = 6.0 Hz, 2H, C*H*-Ar), 7.28-7.17 (m, 12H, C*H*-Ar), 3.60-3.38 (m, 3H), 3.17 (s, 2H), 3.10 (d, *J* = 6.0 Hz, 2H), 2.80-2.06 (m, 20H), 1.46-1.40 (m, 2H), 1.34 (s, 9H), 1.30 (s, 9H). ^{13}C Jmod NMR (75 MHz, CDCl₃, 25 °C, TMS): δ (ppm) = [170.7, 170.6] (*C*O), [149.51, 145.9, 139.5] (*C*-Ar), [129.8, 129.3, 128.9, 128.6, 128.0, 127.9, 126.7, 126.6, 123.0] (*C*H-Ar), [80.3, 80.2] (*C*(CH₃)₃), [60.1, 59.7, 57.5] (CH_2-Ph), [57.04, 56.9, 56.4, 56.0, 52.0, 51.7, 50.9, 49.6] (CH_2-α-N), 36.8 (*C*H-β-N), 37.3 (CH_2-α-N), 27.9 (*C*H₃, × 2), 24.8 (CH_2-β-N). HRMS (ESI) *m/z* calcd for $C_{43}H_{62}N_5O_6^+$ [M+H]⁺: 744.4700; found: 744.4695.

Compound 8. Compound **7** (1.4 mg, 1.88 mmol) was dissolved in absolute EtOH (100 mL). 10 % Pd/C-activated (280 mg) was added and the reaction mixture was stirred under a hydrogen atmosphere at room temperature for 4 days. The mixture was then filtrated through Celite and the solvent was evaporated under reduced pressure to obtain compound **8** as yellow oil (830 mg, 83%). ^{1}H NMR (300 MHz, CDCl₃, 25 °C, TMS): δ (ppm) = 6.74 (d, *J* = 9.0 Hz, 2H, C*H*-Ar), 6.42 (d, *J* = 9.0 Hz, 2H, C*H*-Ar), 3.25 (t, *J* = 12 Hz, 2H), 2.96-

This journal is © The Royal Society of Chemistry 2015

Org. Biomol. Chem. 2015, **00**, 1-3 | **7**

2.11 (m, 21H), 1.87 (bs, 1H), 1.52 (bs, 1H), 1.25 (s, 9H), 1.24 (s, 9H). ^{13}C Jmod NMR (75 MHz, CDCl$_3$, 25 °C, TMS): δ (ppm) = [170.4, 170.3] (*CO*), [144.4, 130.0] (*C*-Ar), [129.7, 115.0] (*CH*-Ar), 80.4 (*C*(CH$_3$)$_3$, × 2), [59.3, 56.0, 55.5] (*CH$_2$*-Ph), [55.0, 54.6, 52.7, 50.7, 47.9, 38.1] (*CH$_2$*-α-N), 37.4(*CH*-β-N), 28.1 (*CH$_3$*, × 2), 26.0 (*CH$_2$*-β-N). HRMS (ESI) *m/z* calcd for C$_{29}$H$_{52}$N$_5$O$_4^+$ [M+H]$^+$: 534.4019; found: 534.4014.

Compound 9. A solution of *tert*-butyl bromoacetate (475 µL, 3.22 mmol) in distilled CH$_3$CN (50 ml) was added dropwise to a suspension of compound **8** (1 g, 1.87 mmol) and K$_2$CO$_3$ (889 mg, 6.43 mmol) in distilled CH$_3$CN (100 ml) at 0 °C. After 18 hours stirring from 0 °C to room temperature, the reaction mixture was filtrated to remove the access K$_2$CO$_3$ and the solvent was evaporated under vacuum. Finally, The resulting yellow oil was purified by flash chromatography on silica gel (CHCl$_3$/MeOH, 99:1-97:3) to give **9** as yellow oil (1.11 g, 78 %). ^{1}H NMR (300 MHz, CDCl$_3$, 25 °C, TMS): δ (ppm) = 6.87 (d, *J* = 9.0 Hz, 2H, C*H*-Ar), 6.514 (d, *J* = 9.0 Hz, 2H, C*H*-Ar), 3.47 (s, 2H), 3.16 (d, *J* = 6 Hz, 8H), 2.66-2.34 (m, 18H), 1.80 (bs, 1H), 1.48 (bs, 1H), 1.37 (s, 18H), 1.36 (s, 19H). ^{13}C Jmod NMR (75 MHz, CDCl$_3$, 25 °C, TMS): δ (ppm) = [171.2, 170.9] (*CO*), [144.1, 130.9] (*C*-Ar), [129.9, 115.0] (*CH*-Ar), [80.5, 80.4] (*C*(CH$_3$)$_3$), [57.7, 57.0, 51.6, 51.1] (*CH$_2$*-Ph, *CH$_2$*-α-N), 39.4 (*CH*-β-N),37.0 (*CH$_2$*-α-N), 28.1 (*CH$_3$*, × 2), 25.3 (*CH$_2$*-β-N). HRMS (ESI) *m/z* calcd for C$_{41}$H$_{72}$N$_5$O$_8^+$ [M+H]$^+$: 762.5381; found: 762.5375.

Compound 10. 1 M solution of *borane tetrahydrofuran* (3.57 mL, 3.57 mmol) was slowly added to a solution of compound **5** (250 mg, 0.357 mmol) in dray THF (10 mL) then the reaction mixture was stirred for 6 days at room temperature. The white solid obtained after solvents removal under reduced pressure was dissolved in 10 ml of 3 M solution of hydrochloride acid and refluxed for one hour. After cooling down to room temperature, the reaction mixture was neutralized using potassium hydroxide pellets. Finally, compound **10** was obtained as yellow oil (193 mg, 96 %) after a liquid-liquid extraction at pH 14 using dichloromethane (3 x 50 ml) followed by drying over MgSO$_4$ and solvents removal under reduced pressure. ^{1}H NMR (300 MHz, CDCl$_3$, 25 °C, TMS): δ (ppm) = 8.14 (d, *J* = 6.0 Hz, 2H, C*H*-Ar), 7.45-7.23 (m, 12H, C*H*-Ar), 3.89-3.70 (m, 3H), 3.58-2.25 (m, 4H), 2.98-2.05 (m, 20H), 1.62-1.52 (m, 2H). ^{13}C Jmod NMR (75 MHz, CDCl$_3$, 25 °C, TMS): δ (ppm) = [149.6, 146.1, 140.6, 139.9] (*C*-Ar), [129.6, 128.9, 127.8, 128.2, 127.9, 126.7, 126.5, 123.3] (*CH*-Ar), [61.6, 59.9, 59.8] (*CH$_2$*-Ph), [58.6, 58.3, 57.4, 57.1, 55.4, 54.2, 54.0, 52.02] (*CH$_2$*-α-N), 42.2 (*CH*-β-N), 39.8 (*CH$_2$*-β-N). HRMS (ESI) *m/z* calcd for C$_{33}$H$_{44}$N$_5$O$_2^+$ [M+H]$^+$: 542.3495; found: 542.3490.

Compound 11. Compound **10** (2.5 g, 4.32 mmol) was dissolved in absolute EtOH (100 mL). 10 % Pd/C-activated (250 mg) was added and the reaction mixture was stirred under a hydrogen atmosphere at room temperature for 4 days. The mixture was then filtrated through Celite and the solvent was evaporated under reduced pressure to obtain compound **11** as yellow oil (1.5 g, 94 %). ^{1}H NMR (300 MHz, CDCl$_3$, 25 °C, TMS): δ (ppm) = 6.64 (d, *J* = 6.0 Hz, 2H, C*H*-Ar), 6.31 (d, *J* = 6.0 Hz, 2H, C*H*-Ar), 3.72 (bs, 4H, NH + NH$_2$), 3.01-1.76 (m, 23H), 1.36-1.24 (m, 2H). ^{13}C Jmod NMR (75 MHz, CDCl$_3$, 25 °C, TMS): δ (ppm) = 144.4 (*C*-Ar), 129.0 (*CH*-Ar), 128.8 (*C*-Ar), 114.45 (*CH*-Ar), [61.9, 59.4, 57.6, 52.8, 52.7, 51.5, 50.3, 46.5, 48.9, 47.3]

(*CH$_2$*), 37.8 (*CH*-β-N), 37.4 (*CH$_2$*-β-N). HRMS (ESI) *m/z* calcd for C$_{19}$H$_{34}$N$_5^+$ [M+H]$^+$: 332.2814; found: 332.2809.

Compound 12. A solution of *tert*-butyl bromoacetate (2.38 mL, 16.13 mmol) in distilled CH$_3$CN (100 ml) was added dropwise to a suspension of compound **11** (3 g, 8.07 mmol) and K$_2$CO$_3$ (4.46 g, 32.26 mmol) in distilled CH$_3$CN (200 ml) at 0° C. After 18 hours stirring from 0 °C to room temperature, the reaction mixture was filtrated to remove access K$_2$CO$_3$ and the solvent was evaporated under vacuum. Finally, The resulting yellow oil was purified by flash chromatography on silica gel (CHCl$_3$/MeOH, 95:5-85:15) to give **12** as yellow oil (3.57 g, 79 %). ^{1}H NMR (300 MHz, CDCl$_3$, 25 °C, TMS): δ (ppm) = 10.11 (bs, 1H), 6.83 (d, *J* = 9.0 Hz, 2H, C*H*-Ar), 6.58 (d, *J* = 9.0 Hz, 2H, C*H*-Ar), 3.90 (bs, 1H), 3.44-1.62 (m, 26H), 1.41 (s, 9H, CH$_3$), 1.39 (s, 9H, CH$_3$). ^{13}C Jmod NMR (75 MHz, CDCl$_3$, 25 °C, TMS): δ (ppm) = [170.4, 169.9] (*CO*), 145.0(*C*-Ar), 129.8 (*CH*-Ar), 129.1 (*C*-Ar), 115.5 (*CH*-Ar), 82.0 (*C*(CH$_3$)$_3$), 81.8 (*C*(CH$_3$)$_3$), [62.2, 60.2, 56.1, 55.9, 55.4, 53.2, 51.6, 51.3, 50.7] (*CH$_2$*), 40.0 (*CH*-β-N), 37.5 (*CH$_2$*), 28.3 (*CH$_3$*), 28.2 (*CH$_3$*), 23.8 (*CH$_2$*-β-N). HRMS (ESI) *m/z* calcd for C$_{31}$H$_{52}$N$_5$O$_4^+$ [M+H]$^+$: 560.4176; found: 560.4170.

Compound 13. Compound **8** (200 mg, 0.74 mmol) was dissolved in a mixture of anhydrous CH$_2$Cl$_2$/TFA 1:1 (6 mL). The solution was stirred at ambient temperature for 2 days then the solvent was evaporated under reduced pressure at room temperature to give brown oil which was dissolved in 2 ml of water then lyophilized. Compound **13**$^.$4TFA was obtained as an off white solid in quantitative yield. ^{1}H NMR (300 MHz, D$_2$O, 25 °C, TMS): δ (ppm) = 7.12 (bs, 4H, C*H*-Ar), 3.42-3.34 (m, 2H), 3.20 (bs, 2H), 3.03-2.13 (m, 19H), 1.68-1.47 (m, 2H. ^{13}C Jmod NMR (75 MHz, D$_2$O, 25 °C, TMS): δ (ppm) = [176.7, 176.5] (*CO*), 140.5 (*C*-Ar), 131.5 (*CH*-Ar), 129.3 (*C*-Ar), 123.9 (*CH*-Ar), [63.6, 58.0, 55.6, 50.6, 50.3, 50.0, 45.2, 36.4] (*CH$_2$*-Ph, *CH$_2$*-α-N), 35.8 (*CH*-β-N), 23.4 (*CH$_2$*-β-N). HRMS (ESI) *m/z* calcd for C$_{21}$H$_{36}$N$_5$O$_4^+$ [M+H]$^+$: 422.2767; found: 422.2762.

Compound 14. Compound **13**$^.$4TFA (100 mg, 114 µmol) dissolved in hydrochloric acid (1 mL, 3 M) and then reacted with a solution of thiophosgene (175 µL, 2.28 mmol) in 1 mL of chloroform overnight at ambient temperature with vigorous stirring. The reaction mixture was washed with chloroform (5 × 1 mL) by vigorous biphasic stirring followed by decanting of the organic phase with a pipette to remove excess thiophosgene. The aqueous phase was lyophilized to give compound **14**$^.$4HCl as off white solid (60 mg, 87 %). HRMS (ESI) *m/z* calcd for C$_{22}$H$_{34}$N$_5$O$_4$S$^+$ [M+H]$^+$: 464.2332; found: 464.2326. IR: $\tilde{v}$ = 2106 cm^{-1} (NCS).

Compound 15. Compound **9** (100 mg, 0.13 mmol) was dissolved in 6 M solution of hydrochloric acid (10 ml). The reaction mixture was refluxed for 18 hours then the water and excess hydrochloric acid were evaporated under reduced pressure to give brown oil which was dissolved in 2 ml of water and lyophilized. Compound **15**$^.$4HCl was obtained as an off white solid in quantitative yield. ^{1}H NMR (300 MHz, D$_2$O, 25 °C, TMS): δ (ppm) = 7.17 (AB system, *J* = 9.0 Hz, 4H, C*H*-Ar), 3.70 (s, 4H), 3.54 (AB system, *J* = 18.0 Hz, 4H), 3.27-2.86 (m, 16H), 2.49 (d, *J* = 6.0 Hz, 2H), 2.30 (bs, 1H), 1.96 (bs, 1H), 1.76 (bs, 1H). ^{13}C Jmod NMR (75 MHz, D$_2$O, 25 °C, TMS): δ (ppm) = [174.6, 173.5] (*CO*), 142.0 (*C*-Ar), 133.5 (*CH*-Ar), 131.1 (*C*-Ar), 126.1

(CH-Ar), [64.0, 58.0, 57.6, 53.3, 52.7, 38.33] (CH$_2$-Ph, CH$_2$-α-N), 35.7 (CH-β-N), 22.5 (CH$_2$-β-N). HRMS (ESI) m/z calcd for C$_{25}$H$_{40}$N$_5$O$_8^+$ [M+H]$^+$: 538.2877; found: 538.2871.

Compound 16. Compound **15**ᐧ4HCl (62 mg, 86 μmol) dissolved in hydrochloric acid (1 mL, 3 M) and then reacted with a solution of thiophosgene (167 μL, 1.73 mmol) in 1 mL of chloroform overnight at ambient temperature with vigorous stirring. The reaction mixture was washed with chloroform (5 × 1 mL) by vigorous biphasic stirring followed by decanting of the organic phase with a pipette to remove excess thiophosgene. The aqueous phase was lyophilized to give compound **16**ᐧ4HCl as an off white solid (53 mg, 85 %). HRMS (ESI) m/z calcd for C$_{26}$H$_{38}$N$_5$O$_8$S$^+$ [M+H]$^+$: 580.2441; found: 580.2436. IR: $\tilde{v}$ = 2113 cm^{-1} (NCS).

Compound 17. Compound **12** (1 g, 1.79 mmol) was dissolved in 6 M solution of hydrochloric acid (50 ml). The reaction mixture was refluxed for 48 hours and then the water and excess hydrochloric acid were evaporated under reduced pressure to give brown oil which was dissolved in 10 ml of water and lyophilized. Compound **17**ᐧ4HCl was obtained as an off white solid in quantitative yield. ^{1}H NMR (300 MHz, D$_2$O, 25 °C, TMS): δ (ppm) = 7.32 (AB system, J = 9.0 Hz, 4H, CH-Ar), 3.89 (m, 4H), 3.53-261 (m, 25H), 2.31 (bs, 1H), 1.73 (bs, 1H), 1.68 (bs, 1H). ^{13}C Jmod NMR (75 MHz, D$_2$O, 25 °C, TMS): δ (ppm) = [175.3, 175.1] (CO), 141.8 (C-Ar), 133.5 (CH-Ar), 131.2 (C-Ar), 126.1 (CH-Ar), [66.5, 65.0, 62.2, 60.7, 57.9, 56.0, 55.9, 51.2, 50.7, 50.4, 49.9, 38.1] (CH$_2$-Ph, CH$_2$-α-N), 33.8 (CH-β-N), 22.2 (CH$_2$-β-N). HRMS (ESI) m/z calcd for C$_{23}$H$_{38}$N$_5$O$_4^+$ [M+H]$^+$: 448.2924; found: 448.2918.

Compound 18. Compound **17**ᐧ4HCl (100 mg, 169 μmol) was dissolved in hydrochloric acid (1.5 mL, 3 M) and then reacted with a solution of thiophosgene (243 μL, 3.18 mmol) in 1.5 mL of chloroform overnight at ambient temperature with vigorous stirring. The reaction mixture was washed with chloroform (5 × 1 mL) by vigorous biphasic stirring followed by decanting of the organic phase with a pipette to remove excess thiophosgene. The aqueous phase was lyophilized to give compound **18**ᐧ4HCl as off white solid (87 mg, 81 %). HRMS (ESI) m/z calcd for C$_{24}$H$_{36}$N$_5$O$_4$S$^+$ [M+H]$^+$: 464.2488; found: 490.2483. IR: $\tilde{v}$ = 2113 cm^{-1} (NCS).

Conjugation/radiolabelling.
Radionuclides production and reagents. Copper-64 dichloride in 0.1 M hydrochloric acid was obtained from ARRONAX cyclotron (Saint-Herblain, France). Radionuclidic purity was determined by gamma spectroscopy using a DSPEC-JR-2.0 type 98-24B HPGE detector (AMETEK) and chemical purity was controlled by ICP-OES with an iCAP 6500 DUO (Thermo Fisher Scientific). For conjugation and radiolabeling, ammonium acetate, sodium phosphate monobasic anhydrous, sodium phosphate dibasic anhydrous and sodium carbonate anhydrous were purchased as TraceSELECT® grade from Fluka Analytical. Sodium citrate dihydrate, ethylenediaminetetraacetic acid tetrasodium salt hydrate SigmaUltra, ethylenediaminetetraacetic acid ACS reagent, Tris(2-carboxyethyl)phosphine hydrochloride (TCEP-HCl) and lyophilized albumine from bovine serum (BSA) were purchased from Sigma-

Aldrich. Sodium hydrogen carbonate Puratronic® and citric acid monohydrate ACS reagent were purchased from Alfa Aesar and Merck KGaA. Water (18.2 MΩ.cm) was obtained from Milli-Q® Gradient system (Millipore).

Characterization and validation of the 9E7.4 antibody. 9E7.4 mAb production was carried out in-house using a hybridoma obtained from mice immunized with a murine CD-138 epitope-like peptide. This antibody, characterized as a rat IgG2a,κ, was initially validated by ELISA using the 40 aa peptide (data not shown). The specific binding of this 9E7.4 mAb was confirmed by flow cytometry on 5T33 Multiple Myeloma cell line. Flow cytometry data are presented in Figure S44. The 9E7.4 mAb binding affinity onto the 5T33 MM cells is 2.3×10^{-10} M (data not shown).

General procedures. The 9E7.4 mAb solution was depleted of metals by adding 0.2 mL of EDTA 10 mM pH 4.5 solution to 10 mg of antibody (67 nmol; 2 mL; 5 mg/mL) in phosphate buffer salin 0.1 M pH 7. After 2 h of incubation, EDTA was removed and 9E7.4 was transferred in carbonate buffer (pH 8.5, 0.3 M) by ultrafiltration at 2,000 g using a disposable Amicon Ultracel®- 30K filter (Millipore). The 9E7.4 concentration was adjusted to 4-5 mg/mL with same carbonate buffer and measured with a NanoDrop® 1000 UV-vis spectrophotometer (Thermo Fisher Scientific).
For conjugation, the compound **14** was dissolved in carbonate buffer 0.3 M pH 8.5 at the concentration of 12 mg/mL. Immediately after, 1031 μg (670 nmol; 86 μl; 20 molar excess) of **14** were added to 5 mg (33.5 nmol; 1 mL) of 9E7.4 antibody in carbonate buffer 0.3M pH 8.5. The mixture was incubated with gentle stirring overnight at RT and then purified on a PD-10 disposable gel filtration column (GE Healthcare Life Science) eluted with 0.3 M ammonium acetate (pH 7) fractions of 500 μL. In these conditions, molecules with molecular weight below than 10 kD are eluted with a retention volume of 5 to 10 mL and antibody molecules with a retention volume of 2.5 to 4 mL. The fractions corresponding to the immunoconjugate were collected and concentrated to 4 mg/mL using previously described ultrafiltration system.
The purified 9E7.4-CSN-Ph-te2a was then controlled in order to determine the ligand-to-antibody ratio using UPLC-ESI-QTOF analysis. The purified immunoconjugate was injected both in its native or reduced form (mixture of heavy and light chains). In order to reduce the immunoconjugate, 25 μg of 9E7.4-CSN-Ph-te2a (0.17 nmol) were diluted in water to adjust the concentration to 100 μg/ml. Immunoconjugate solution was mixed with TCEP-HCl 100 mM in water at ratio 1:1 V/V and incubated 20 min at RT. UPLC system consists of AcquityH UPLC® bioSample and bioQuaternary solvent managers, an Acquity BEH300 C4 (1.7 μm; 2.1x50 mm) column and a Synapt G2 QTOF (Waters S.A.S. France). Eluents consists of 5 % acetonitrile in water with 0.1% of formic acid (eluent A) and 100 % acetonitrile with 0.1% of formic acid (eluent B). The elution gradient applied to the system was the following: 95 % of eluent A over 1 min, 5 % to 95 % enrichment of eluent B for 6 min, 1 min plateau (95 % of eluent B) and a return to the initial conditions in 2 min flow-rate: 0.6 mL/min; column heated at 80 °C. MS acquisition was performed in ESI positive mode (3kV) and results were analyzed using Waters MassLynxTM software.
For both te2a-Ph-NCS **14** and 9E7.4-CSN-Ph-te2a radiolabeling optimization, the conditions used are presented in Table S1 (see in ESI). Radiolabeling was performed using the following methodology. Briefly, 5μL of copper-64 solution (specific activity

This journal is © The Royal Society of Chemistry 2015

Org. Biomol. Chem. 2015, **00**, 1-3 | **9**

relative to natural copper: 24.75 MBq/nmol; specific activity relative to total metal: 6.8 MBq/nmol; volumic activity: 1.1 GBq/mL at calibration time) were added to 40 µL of 0.3 M ammonium acetate (pH 7) or 0.3 M acetate buffer (pH 5). Then, 1.1 molar equivalent of 9E7.4-CSN-te2a (222 pmol; 8.3 µL ; 4 mg/mL ; 26.7 nmol/mL) or te2a-Ph-NCS (222 pmol; 8,9 µL ; 38.5 µg/mL ; 25 nmol/mL) in ammonium acetate 0.3 M (pH7) were added to copper-64 solution and the mixture was incubated in 1 mL Eppendorf plastic tube. After 5 min incubation, a TLC was performed on PALL ITLC-SG with 0.1 M citrate buffer pH 4.5 as eluent for 9E7.4-CSN-te2a or silica gel (TLC-PET foils, Fluka analytical) using a mixture of ammonium acetate (10% in water) and methanol (1:1) as eluent for te2a-Ph-NCS. For both TLC technics, radioactive distribution was revealed on a storage phosphor screen using a Cyclone Plus phosphor imager (Perkin-Elmer).

A competition assay was conducted by adding 22 µL (2.2 µmol; 10000 eq.) of 0.1 M EDTA pH 7 solution to both radiolabeled antibody conjugate (222 pmol) and unconjugated radiolabeled ligand (222 pmol).

The best condition of radiolabeling has been selected for the scale up radiolabeling used for the in vivo study. For this purpose, 55µL of 2.5 M ammonium acetate solution were added to 300 MBq (273 µL) of copper-64 solution in order to obtain a pH close to 7. Then 1.1 molar equivalent of 9E7.4-CSN-te2a (12.12 nmol ; 454 µL ; 4 mg/mL; 26.7 nmol/mL) in 0.3 M ammonium acetate (pH 7) were added and the mixture was incubated at 40°C during 30 min. To stop the complexation reaction, 10 µl of 10 mM EDTA pH 7 solution was introduced and, after 5 min incubation at 40°C, a TLC was performed in the same conditions as described above. Following the radiolabeling, the raw ^{64}Cu-9E7.4-CSN-te2a solution was purified on PD-10, eluted with 0.1 M phosphate buffer saline pH 7.2 (PBS) by using the same methodology as described before for the antibody conjugation. Radioactivity of the purified recovered radioimmunoconjugate was measured with a calibrated Scintidose^{TM} activimeter (Lemerpax) to assess the radiolabeling yield and specific activity of the purified radioimmunoconjugate. Radiochemical purity of the purified radioimmunoconjugate was measured on ITLC-SG plate as describe for the optimization of radiolabeling.

The ^{64}Cu-9E7.4-CSN-te2a immunoreactivity was assessed by incubating 2 samples (0.5 and 1 pmol) with 200 µg of Pierce™ NHS-activated magnetic beads grafted with a murine CD-138 epitope-like peptide (50 µg for 10 mg of beads). To avoid nonspecific coating of the radioimmunoconjugate on the Eppendorf tube, 100 µl of 0.1 M phosphate buffer/BSA 0.5 % was added to the mixture and followed by 1 h incubation at RT under stirring. Then, beads and supernatant were separated using a magnetic rack (MagRack 6, GE Healthcare Life Science). Beads were rinsed with 200 µl of 0.1 M phosphate buffer pH 7.2/BSA 0.5 %. The supernatant and rinsing solution was pooled, the beads were suspended again with 200 µL of phosphate buffer pH 7.2 and these latters were counted using a Wallac 1480-Wizard™ 3 gamma counter (Perkin Elmer). The immunoreactivity, expressed as a percentage, was calculated as the counts per minute (CPM) for the beads divided by the sum of the CPM for the beads, the supernatant and the rinsing solution and the remaining activity in the tube.

In vivo PET study on multiple myeloma mice model. Animal experiments were carried out in compliance with French regulation. The protocol was approved by the Ministère de l'Enseignement Supérieur et de la Recherche (No. 00143.02) following its evaluation by an ethics committee for animal experimentation. A set of five mature (14 weeks old) female C57BL/KaLwRij mice was purchased from Harlan CPB France. Mice were housed under standard conditions, standard diet and water ad libitum.

Murine myeloma 5T33 cell line was kindly provided by Dr. Harvey Turner (Nuclear Medicine Department, Fremantle Hospital, Australia), with permission of Dr. Jiri Radl (TNO Institute, Leiden, The Netherlands).[61] Cells were transfected with luciferase cDNA as described previously.[62]

Mice were injected subcutaneously (dorsal) with 1 million 5T33-Luc(+) cells. For PET imaging purposes, 5T33-Luc(+) tumor bearing mice were injected into a tail vein with ^{64}Cu-9E7.4-CSN-te2a (7-9 MBq), 13-15 days post-graft. At 2 and 20 h post-injection, animals were anaesthetized with 2.5 % isoflurane and 50 % O_2 in air and placed on the bed of a Inveon™ PET-CT (Siemens Medical Solutions, Knoxville, USA) and imaged over 20 min. The images were reconstructed using 3D/OSEM (2 iterations) followed by MAP (18 iterations) algorithms. Post-treatment imaging was performed with Siemens Inveon Research Workplace software. The biodistribution data were obtained by direct quantification of the in vivo PET images.

Notes and references

1   T. J. Wadas, E. H. Wong, , G. R. Weisman, C. J. Anderson, *Curr. Pharmaceutical Design,* 2007, **13**, 3.

2   T. J. Wadas, E. H. Wong, , G. R. Weisman, C. J. Anderson, *Chem. Rev.*, 2010, **110**, 2858.

3   R. Delgado, V. Felix, L. M. P. Lima, D. W. Price, *Dalton Trans.,* 2007, 2734.

4   C. A. Boswell, X. Sun, W. Niu, G. R. Weisman, E. H. Wong, , A. L. Rheingold, C. J. Anderson, *J. Med. Chem.*, 2004, **47**, 1465.

5   J. C. Garrison, T. L. Rold, G. L. Sieckman, S. D. Figueroa, W. A. Volkert, S. S. Jurisson, T. J. Hoffman, *J. Nucl. Med. Off. Publ. Soc. Nucl. Med.,* 2007, **48**, 1327.

6   J. E. Sprague, Y. Peng, X. Sun, G. R. Weisman, E. H. Wong, S. Achilefu, C. J. Anderson, *Clin. Cancer Res. Off. J. Am. Assoc. Cancer Res.*, 2004, **10**, 8674.

7   D. N. Pandya, N. Bhatt, A. V. Dale, , J. Y. Kim, H. Lee, Y. S. Ha, J.-E. Lee, G. I. An, J. Yoo, *Bioconjug. Chem.*, 2013, **24**, 1356.

8   T. J. Wadas, E. H. Wong, G. R. Weisman, C. J. Anderson, *Chem. Rev.*, 2010*, **110**, 2858.

9   L. R. Gahan, J. M. Harrowfield, Polyhedron, 2015, **94**, 1.

10 A. M. Sargeson, *Coord. Chem. Rev.*, 1996*, **151**, 89.

11 N. Di Bartolo, A. M. Sargeson, S. V. Smith, *Org. Biomol. Chem.* 2006, **4**, 3350.

12 A. F Prasanphanich, P. K. Nanda, T. L. Rold, L. Ma, M. R. Lewis, J. C. Garrison, T. J. Hoffman, G. L. Sieckm, S. D. Figueroa, C. Smith, *J. Proc. Natl. Acad. Sci. U.S.A.*, 2007, **104**, 12462.

13 D. Liu, D. Overbey, L. D. Watkinson, C. J. Smith, S. Daibes-Figueroa, T. J. Hoffman, L. R. Forte, W. A. Volkert, M. F. Giblin, *Bioconjug. Chem.*, 2010, **21**, 1171.

14 R. A. Dumont, F. Deininger, R. Haubner, H. R. Maecke, W.A. Weber, M. Fani, *J. Nucl. Med. Off. Publ. Soc. Nucl. Med.*, 2011, **52**, 1276.

15 S. Juran, M. Walther, H. Stephan, R. Bergmann, J. Steinbach, W. Kraus, F. Emmerling, P. Comba, *Bioconjug. Chem.*, 2009, **20**, 347.

16 C. A. Boswell, C. A. S. Regino, K. E. Baidoo, K. J. Wong, A. Bumb, H. Xu, D. E. Milenic, J. A. Kelley, C. C. Lai, M. W. Brechbiel, *Bioconjugate Chem.,* 2008, **19**, 1476.

17 D. N. Pandya, J. Y. Kim, J. C. Park, H. Lee, , P. B. Phapale, W. Kwak, T. H. Choi, G. J. Cheon, Y.-R. Yoon, J. Yoo, *Chem. Commun.* 2010, **46**, 3517.

18 E. A. Lewis, R. W. Boyle, S. J. Archibald, *Chem. Commun.*, 2004, 2212.

19 R. Ferdani, D. J. Stigers, A. L. Fiamengo, L. Wei, B. T. Y. Li, J. A. Golen, A. L. Rheingold, G. R. Weisman, E. H. Wong, C. J. Anderson, *Dalton Trans.*, 2012, **41**, 1938.

20 D. J. Stigers, R. Ferdani, G. R. Weisman, E. H. Wong, C. J. Anderson, J. A. Golen, M. Curtis, A. L. Rheingold, *Dalton Trans.*, 2010, **39**, 1699.

21 C. A. Boswell, C. A. S. Reginob, K. E. Baidooa, K. J. Wong, D. E. Milenic, J. A. Kelley, C. C. Lai, M. W. Brechbiel, *Bioorg. Med. Chem.*, 2009, **17**, 548.

22 L. M. P. Lima, D. Esteban-Gómez, R. Delgado, C. Platas-Iglesias, R. Tripier, *Inorg. Chem.*, 2012, **51**, 6916.

23 M. Frindel, N. Camus, A. Rauscher, M. Bourgeois, C. Alliot, L. Barré, J.-F. Gestin, R. Tripier, A. Faivre-Chauvet, *Nucl. Med. Biol*, 2014, **41**, 49.

24 L. M. P. Lima, Z. Halime, N. Camus, R. Marion, R. Delgado, C. Platas-Iglesias, R. Tripier, *Inorg. Chem.*, 2014, **53**, 5269.

25 D. N. Pandya, J. Y. Kim, J. C. Park, H. Lee, P. B. Phapale, W. Kwak, T. H. Choi, G. J. Cheon, Y.-R. Yoon, J. *Chem. Commun.* 2010, **46**, 3517.

26 E. T. Clarke, A. E. Martell, *Inorg. Chim. Acta*, 1991, **190**, 27.

27 R. Delgado, J. J. R. F. Da Silva, *Talanta*, 1982, **29**, 815.

28 K. S. Woodin, K. JHeroux, C. A. Boswell, E. H. Wong, G. R. Weisman, W. Niu, S. A. Tomellini, C. J. Anderson, L. N. Zakharov and A. R. Rheingold, *Eur. J. Inorg. Chem.,* 2005, 4829.

29 K. J. Heroux, K. S Woodin, D. J. Tranchemontagne, P. C. B. Widger, E. Southwick, E. H. Wong, G. R. Weisman, S. A. Tomellini, T. J. Wadas, C. J. Anderson et al., *Dalton Trans.*, 2007, 2150.

30 X. Sun; M. Wuest, G. R. Weisman, E. H.,Wong, D. P. Reed, C. A. Boswell, R. Motekaitis, A. E. Martell, M. J. Welch, C. J. Anderson, *J. Med. Chem.* 2002, **45**, 469.

31 A. Y. Lebedev, J. P. Holland, J. S. Lewis, *Chem. Commun.*, 2010, **46**, 1706.

32 J. D. Silversides, R. Smith, S. J. Archibald, *Dalton Trans.*, 2011, **40**, 6289.

33 J. E. Sprague, Y. Peng, A. L. Fiamengo, K. S. Woodin, E. A. Southwick, G. R. Weisman, E. H. Wong, J. A. Golen, A. L. Rheingold, C. J. Anderson, *J. Med. Chem.*, 2007, **50**, 2527.

34 W. Liu, G. Hao, M. A. Long, T. Anthony, J.-T. Hsieh, X. Sun, *Angew. Chem. Int. Ed.*, 2009, **48**, 7346.

35 C. A. Boswell, C. A. S. Regino, K. E. Baidoo, K. J. Wong, A. Bumb, H. Xu, D. E. Milenic, J. A. Kelley, C. C. Lai, M. W. Brechbiel, *Bioconjugate Chem.* 2008, **19**, 1476.

36 P. V. Bernhardt and G. A. Lawrance, *Coord. Chem. Rev.*, 1990*, **104***, 297.

37 S. Liu, *Adv. Drug Deliv. Rev.*, 2008, **60**, 1357.

38 X. Liang, P. J. Sadler, *Chem. Soc. Rev.*, 2004, **33**, 246.

39 M. K. Moi, C. F. Meares, M. J. McCall, W. C. Cole, S. J. DeNardo, *Anal. Biochem.*, 1985, **148**, 249.

40 M. J. McCall, H. Diril, C. F. Meares, *Bioconjug. Chem.*, 1990, **1**, 222.

41 D. N. Pandya, J. Y. Kim, W. Kwak, J. C. Park, M. B. Gawande, G. I. An, E. K. Ryu, J. Yoo, *J. Nucl. Med. Mol. Imaging*, 2010, **44**, 185.

42 N. Camus, Z. Halime, H. Bernard, N. Le Bris, C. Platas-Iglesias, R. Tripier, *J. Org. Chem.*, 2014, **79** (5), 1885.

43 Tripier, R. ; Camus, N. World Patent, **2013**, WO 2013072491 A1.

44 D. L. Kukis, H. Diril, D. P. Greiner, S. J. DeNardo, G. L. DeNardo, Q. A. Salako, C. F. Meares, *Cancer Supplement*, 1993, **73**, 779.

45 J. K. Moran, D. P. Greiner, C. F. Meares, *Bioconjugate Chem.*, 1995, **6**, 296.

46 P. Moreau, M. Tinkl, M. Tsukazaki, P. S. Bury, E. J. Griffen, V. Snieckus, R. B. Maharajh, C. S. Kwok, V. V. Somayaji, Z. Peng, T. R. Sykes, A. A. Noujaim, *Synthesis*, 1997, 1010.

47 E. A. Lewis, C. C. Allan, R. W. Boyle, S. J. Archibald, *Tetrahedron Letters*, 2004, **45**, 3059.

48 T. Derlin, P. Bannas, *World J Orthop.*, 2014, **5**(3), 272.

49 E. W. Price, B. M. Zeglis, J. F. Cawthray, C. F. Ramogida, N. Ramos, J. S. Lewis, M. J. Adam, C. Orvig, *J. Am. Chem. Soc.*, 2013, **135** (34), 12707.

50 D. R. B. Vera, S. Eigner, K. E. Henke, O. Lebeda, F. Melichar and M. Beran, *Nucl. Med. Biol.*, 2012, **39**.

51 C. Wu, E. Jagoda, M. Brechbiel, K. O. Webber, I. Pastan, O. Gansow and W. C. Eckelman, *Bioconjug. Chem.*, 1997, **8**, 365.

52 A. M. Wu, P. J. Yazaki, S. W. Tsai, K. Nguyen, A. L. Anderson, D. W. McCarthy, M. J. Welch, J. E. Shively, L. E. Williams, A. A. Raubitschek et al. *Proc. Natl. Acad. Sci. U. S. A.*, 2000, **97**, 8495.

53 S. C. Ghosh, K. L. Pinkston, H. Robinson, B. R. Harvey, N. Wilganowski, K. Gore, E. M. Sevick-Muraca, A. Azhdarinia, *Nucl. Med. Biol.,* 2015, **42**, 177.

54 C. Schjoeth-Eskesen, C. H. Nielsen, S. Heissel, P. Højrup, P. R. Hansen, N. Gillings, A. Kjaer, *J. Label. Compd. Radiopharm.*, 2015, **58**, 227.

55 K. Alt, B. M. Paterson, K. Ardipradja, C. Schieber, G. Buncic, B. Lim, S. S. Poniger, B. Jakoby, X. Wang, G. J. O'Keefe, H. J. Tochon-Danguy, A. M. Scott, Ackermann U, Peter K, P. S. Donnelly, C. E. Hagemeyer, *Mol. Pharm.*, 2014, **11**, 2855.

56 D. Zeng, Y. Guo, A. G. White, Z. Cai, J. Modi, R. Ferdani, C. J. Anderson, *Mol. Pharm.*, 2014, **11**, 3980.

57 K. I. Stanford, J. R. Bishop, E. M. Foley, J. C. Gonzales, I. R. Niesman, J. L. Witztum, J. D. Esko, *J. Clin. Invest.*, 2009, **119**, 3236.

58 L. A. Bass, M. Wang, M. J. Welch, C. J. Anderson, *Bioconjug. Chem.*, 2000, **11**, 527.

59 B. E. Rogers, C. J. Anderson, J. M. Connett, L. W. Guo, W. B. Edwards, E. L. Sherman, K. R. Zinn, M. J. Welch, *Bioconjug. Chem.*, 1996, **7**, 511.

60 G. R. Mirick, R. T. O'Donnell, S. J. DeNardo, S. Shen, C. F. Meares, G. L. DeNardo, *Nucl. Med. Biol.*, 1999, **26**, 841.

61 J. Radl, J. W. Croese, C. Zurcher, M. H Van den Enden-Vieveen, A. M. de Leeuw, *Am. J. Pathol.*, 1988, **132**, 593.

62 M. Onishi, S. Kinoshita, Y. Morikawa, A. Shibuya, J. Phillips, L. L. Lanier, D. M. Gorman, G. P. Nolan, A. Miyajima, T. Kitamura, *Exp. Hematol.*, 1996, **24**, 324.

12 | *Org. Biomol. Chem*. 2015, **00**, 1-3

This journal is © The Royal Society of Chemistry 2015

Organic & Biomolecular Chemistry Accepted Manuscript